

## Electronic Supplementary Information File

### Table of Contents

1. Detailed description of the instrumentation features, computational details and SHG experimental setups	2
2. $^1\text{H}$ and $^{13}\text{C}$ NMR spectra	5
3. Experimental electronic absorption spectra of the chromophores <b>EDBA-VQV-TCF</b> (a), <b>HODEA-VQV-TCF</b> (b) (Fig. S1)	15
4. DSC curves for chromophores <b>DBA-VQV-TCF</b> (Fig. S2)	16
5. DSC curves for chromophores under studied (Fig. S3)	17
6. The notation of the bonds around which rotation is realized (Fig. S4) and <b>DBA-VQV-TCF</b> conformers (Fig. S5)	18
7. Dihedral angles between moiety planes of studied chromophores (Table S1)	19
8. Frontier orbitals calculated at B3LYP/6-31G* level of studied chromophores (Fig. S6)	20
9. UV-vis electron absorption spectra for films before and after poling (Fig. S7, S8)	22
10. NLO coefficients ( $d_{33}$ ), order parameters ( $\eta$ ), poling temperature ( $T_p$ ), $\lambda_{\text{max}}$ of polymer film and film thickness ( $h$ ) for composite materials under study (Table S2, S3)	24

### Detailed description of the instrumentation features, computational details and SHG experimental setups

NMR experiments were performed with Bruker AVANCE-600, AVANCE-500 and AVANCE-400 (600 MHz, 500 MHz and 400 MHz for  $^1\text{H}$  NMR, 150 MHz, 125 MHz and 100 MHz for  $^{13}\text{C}$  NMR) spectrometers. Chemical shifts ( $\delta$  in ppm) are referenced to the solvents. Infrared (IR) spectra were recorded on the Bruker Vector-22 FT-IR spectrometer. The mass spectra were obtained on Bruker UltraFlex III MALDI TOF/TOF instrument with *p*-nitroaniline as a matrix. UV–vis spectra were recorded at room temperature on a UV-6100 Ultraviolet/Visible Spectrophotometer using 10 mm quartz cells. Spectra were registered with a scan speed of 480 nm/min, using a spectral width of 1 nm. All samples were prepared in solution with the concentrations of ca  $\sim 3 \times 10^{-5}$  mol/L. The melting points, mp, of chromophores were determined by Melting Point Meter MF-MP-4. The thermal stabilities of chromophores were investigated by simultaneous thermal analysis (thermogravimetry/differential scanning calorimetry - TG/DSC) using NETZSCH (Selb, Germany) STA449 F3 instrument. Approximately 3–4 mg samples were placed in an Al crucible with a pre-hole on the lid and heated from 30 to 500 °C. The same empty crucible was used as the reference sample. High-purity argon was used with a gas flow rate of 50 mL/min. TG/DSC measurements were performed at the heating rates of 10 K/min. The thickness of doped polymer films was determined by AFM technique by a dimension FastScan high-resolution scanning probe microscope (Bruker, Germany). Ultra-sharp silicon probes Bruker ScanAsyst-air with a tip curvature radius of  $\sim 2$  nm were used. Organic solvents used were purified and dried according to standard methods. The reaction progress and the purity of the obtained compounds were controlled by TLC on Sorbfil UV-254 plates with visualization under UV light.

The electric properties of the studied chromophores are calculated by the (TD)DFT at the M06-2X/aug-cc-pVDZ level with chromophore geometry fully optimized at the B3LYP/6-31G\* level. The M06-2X density functional is shown to provide reliable estimations of molecular polarizabilities of dipole chromophores with heterocyclic fragments in  $\pi$ -conjugated bridge<sup>29a</sup>, in particular, those with quinoxaline moiety in  $\pi$ -electron bridge<sup>20a</sup>. Calculations were performed using Jaguar program package<sup>29b,c</sup>. The atomistic modeling was performed for chromophores **BODEA-VQV-TCF** and **EDBA-VQV-TCF** in gas phase in the energy window 5 kcal/mol with OPLS4 force field<sup>30</sup>; a conformational search allowed to reveal the most stable conformers which structure was chosen as starting point for quantum chemical geometry optimization. The modeling was performed with MacroModel program<sup>31</sup>.

### Nonlinear optical response measurements

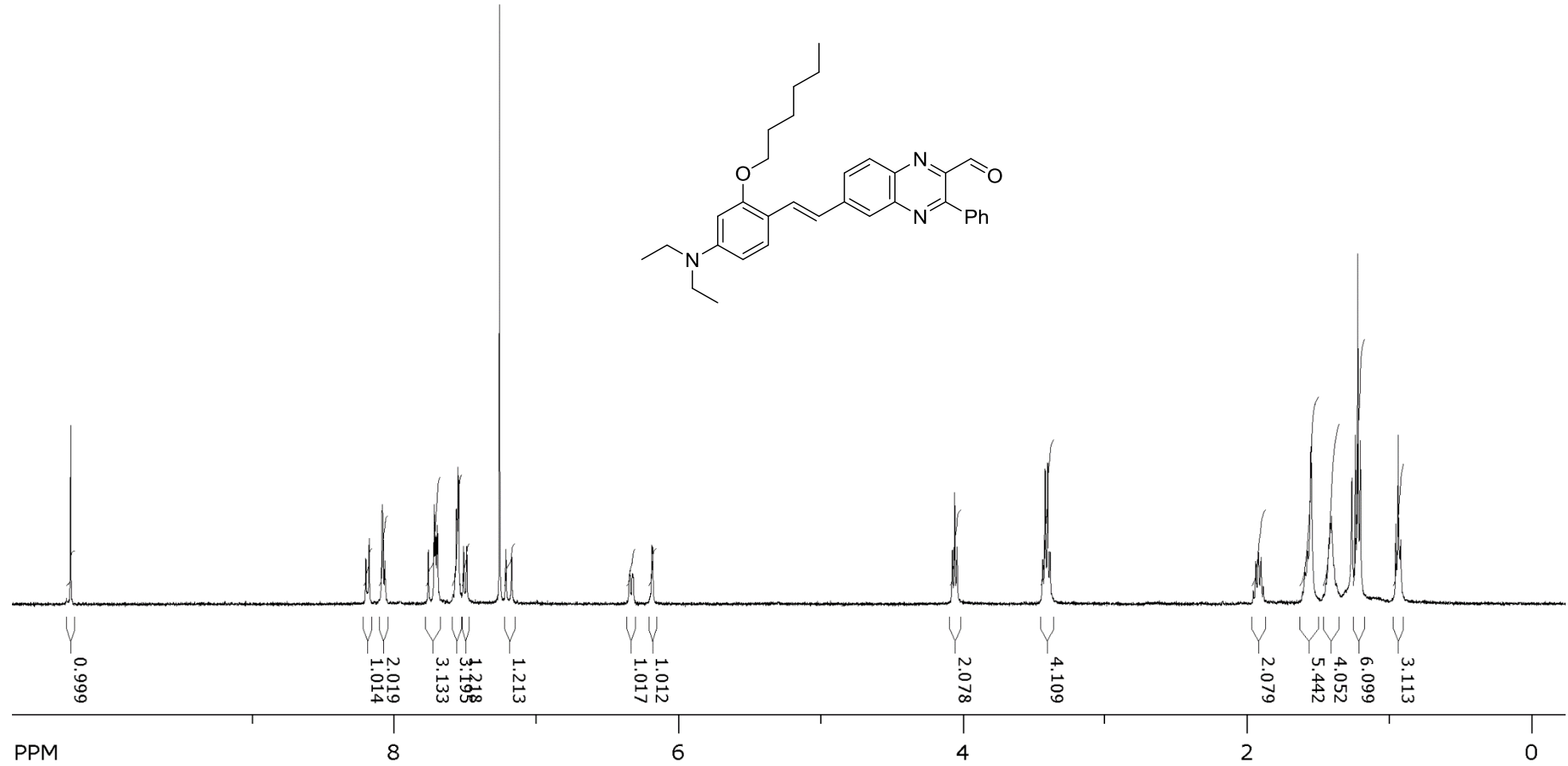
Second order NLO coefficients were measured by two different approaches:

1. SHG was performed by the femtosecond amplified laser system which allowed measuring the SHG intensity emitted by the sample without any micro-objective or another focusing system. The laser system produced pulses with the following parameters: the wavelength is 1028 nm, the pulse repetition rate is 3 kHz, pulse duration is 200 fs, a pulse energy is 164  $\mu$ J, and mean power of the laser beam is 492 mW. The beam diameter of 3 mm resulted in the peak pulse intensity of about 11.6 GW/cm<sup>2</sup>. SHG intensity was measured using  $\alpha$ -quartz crystal as a source of a reference signal. The NLO coefficient of the sample  $d_{33,s}$  was estimated as follows<sup>27a</sup>:  $\frac{d_{33,s}}{d_{11,q}} = \sqrt{I_s/I_q} \frac{l_{c,q}}{l_s} F$ , where  $d_{11,q}$  is known quartz nonlinear coefficient (0.45 pm/V),  $I_s$  and  $I_q$  are SHG intensities produced by the sample and the quartz, respectively, and measured in the same configuration,  $l_{c,q}$  is quartz coherence length related to 1028 nm (calculated as 13  $\mu$ m),  $l_s$  is sample thickness,  $F$  is correction factor (1.2 when  $l_{c,q} \gg l_s$ )<sup>27b</sup>. It was assumed in analyzing experimental data that  $d_{33}/d_{13} \approx 3$ . This approach does not require knowledge of the exact values of the complex refractive index of the samples, which greatly simplifies obtaining information about the material NLO properties. This approach is also quite useful for relative measurements of the NLO response of different samples with similar parameters (absorption spectra, film thickness).

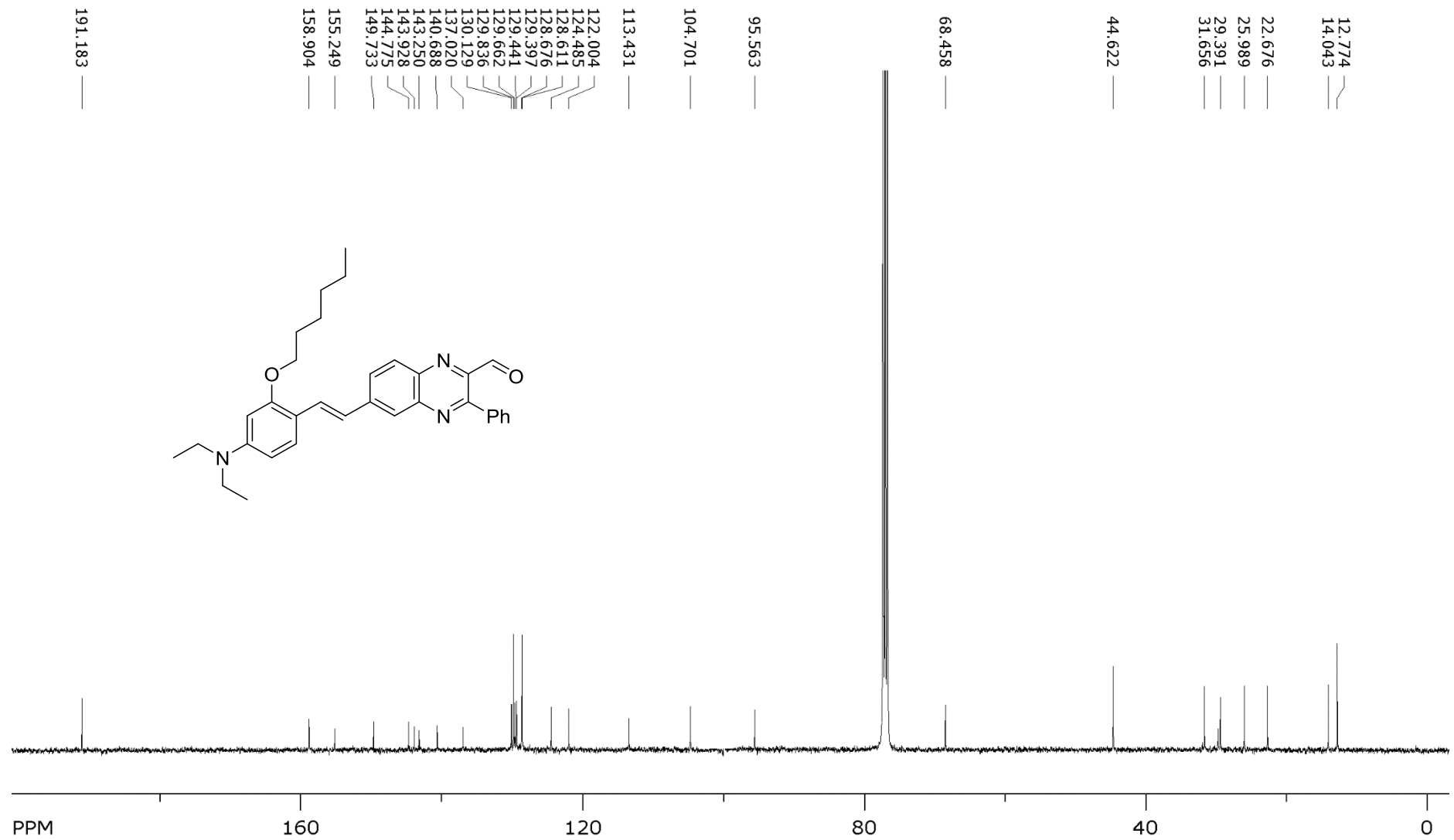
2. For a more precise determination of the quadratic NLO coefficients  $d_{33}$  we used Maker fringes technique with theoretical approach given by<sup>28a</sup>, which accurately takes into account the absorption and polarization of radiation. Nanosecond laser pulses were used for an optical excitation (“Solar LS” LQ529A-LP601, 1064 nm, 3 mJ, 10 ns, 10 Hz repetition rate) of a sample on a rotating stage located in the focus of a Keplerian telescope. A focal length of the telescope lenses was chosen to obtain a tradeoff between the power density on the sample ( $\sim 0.3$  GW/cm<sup>2</sup>) and a distortions pattern of the angular dependence of the second harmonic signal under rotation of a sample. SHG intensity was measured in the S-P field configuration<sup>28b</sup> (the symbols indicate S- or P-type of the polarization relative to the plane of incidence on the sample for the exciting or detected radiation, respectively). 1 mm thick quartz plate was used as a reference (Y-cut, p-p configuration,  $d_{11} = 0.45$  pm/V<sup>28c</sup>) similarly to<sup>28b</sup>. In order to obtain  $d_{33}$  coefficients of samples it is required to know their complex refractive indices. The extinction coefficients at a wavelength of 532 nm were determined from the optical density spectra with known thickness of the sample. Refractive indices were measured at individual wavelengths (517.1, 532.0, 635.9, 846.4, 1309.6, and 1537.5 nm using a Prism coupler Metricon model 2010/M system). The measurement error was taken equal to 0.003. The refractive

index at a wavelength of 1064 nm was estimated by polynomial interpolation of experimental values measured in the IR region, far from the absorption bands.

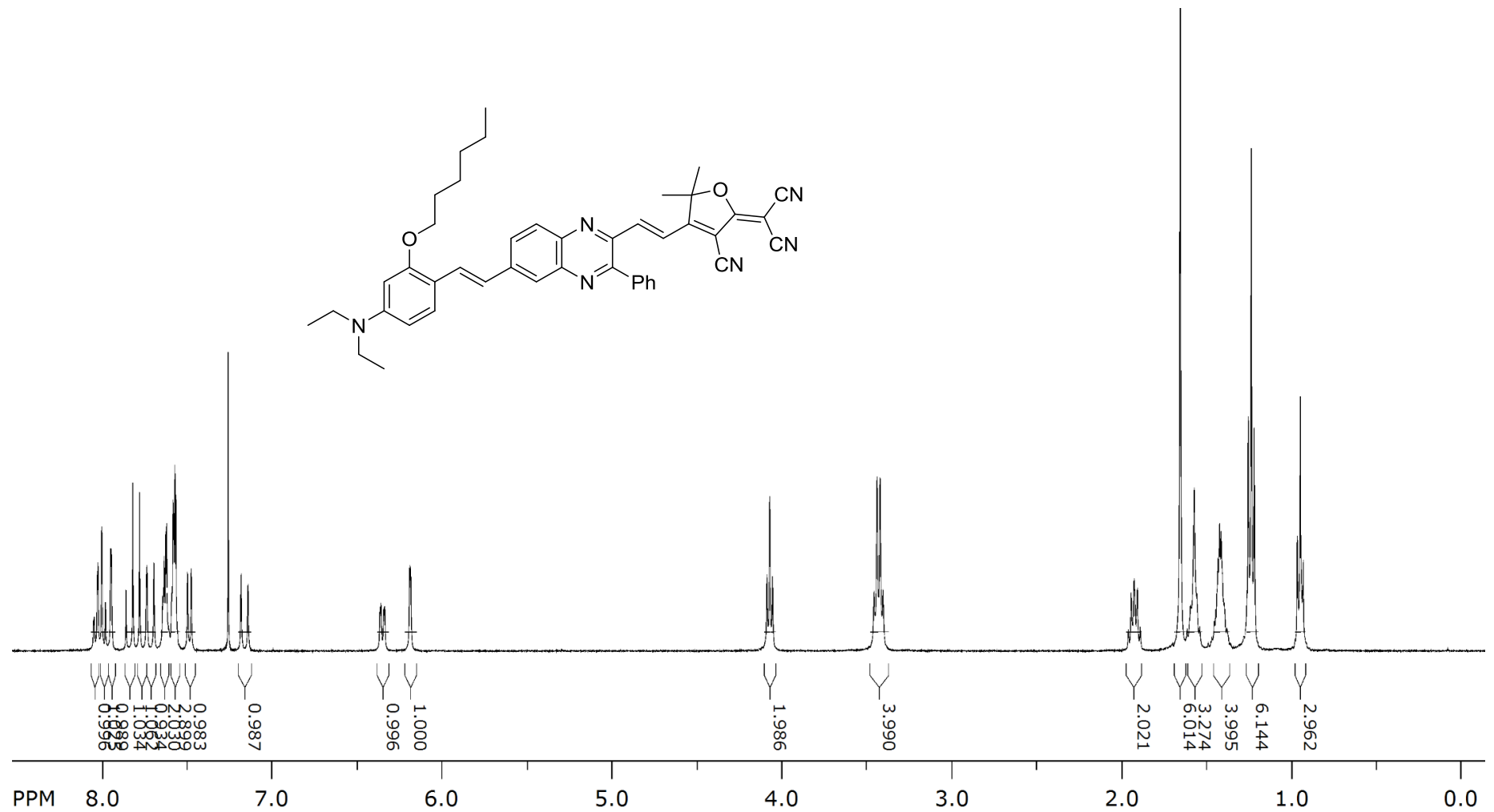
3. Samples **DBA-VQV-TCF(25)/PMMA** and **EDBA-VQV-TCF(30)/PMMA** were selected for  $d_{33}$  measurements at heating to characterize the resistance of  $d_{33}$  to temperature increase. The intensity of second harmonic was recorded while the sample was heated. Sample was fixed at a proper angle of incidence of the laser beam and a heating rate of 50 °C/min was chosen to provide sufficient measurement time at the current temperature. Such heating rate is slow enough to uniform sample heating and fast enough to show residual NLO response during short-term heating of the sample. The temperature measurement accuracy was  $\pm 2$  °C.

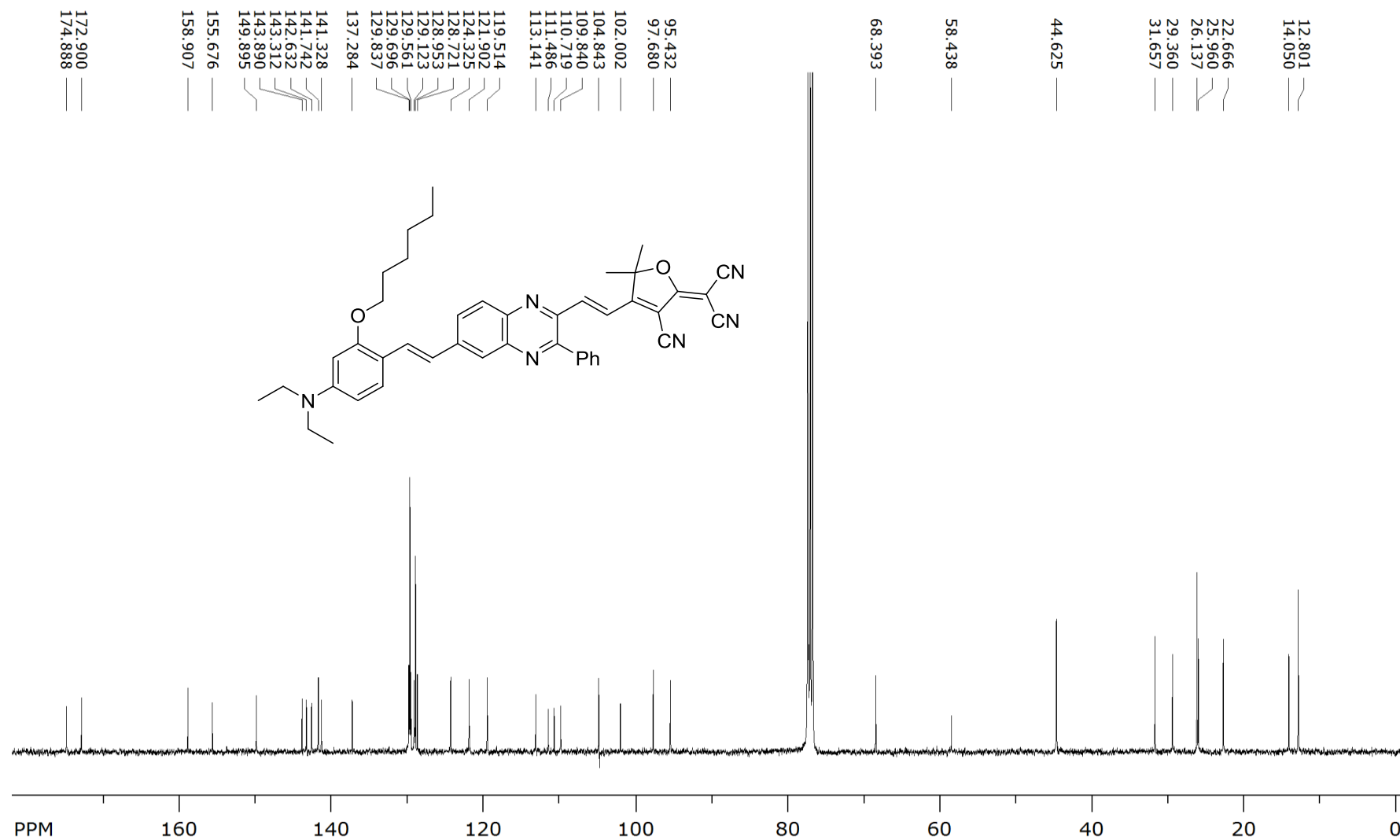


<sup>1</sup>H NMR spectrum (CDCl<sub>3</sub>, 400 MHz) of (*E*)-6-(4-(*N,N*-diethylamino)-2-(hexyloxy)styryl)-3-phenylquinoxaline-2-carbaldehyde (**4c**)



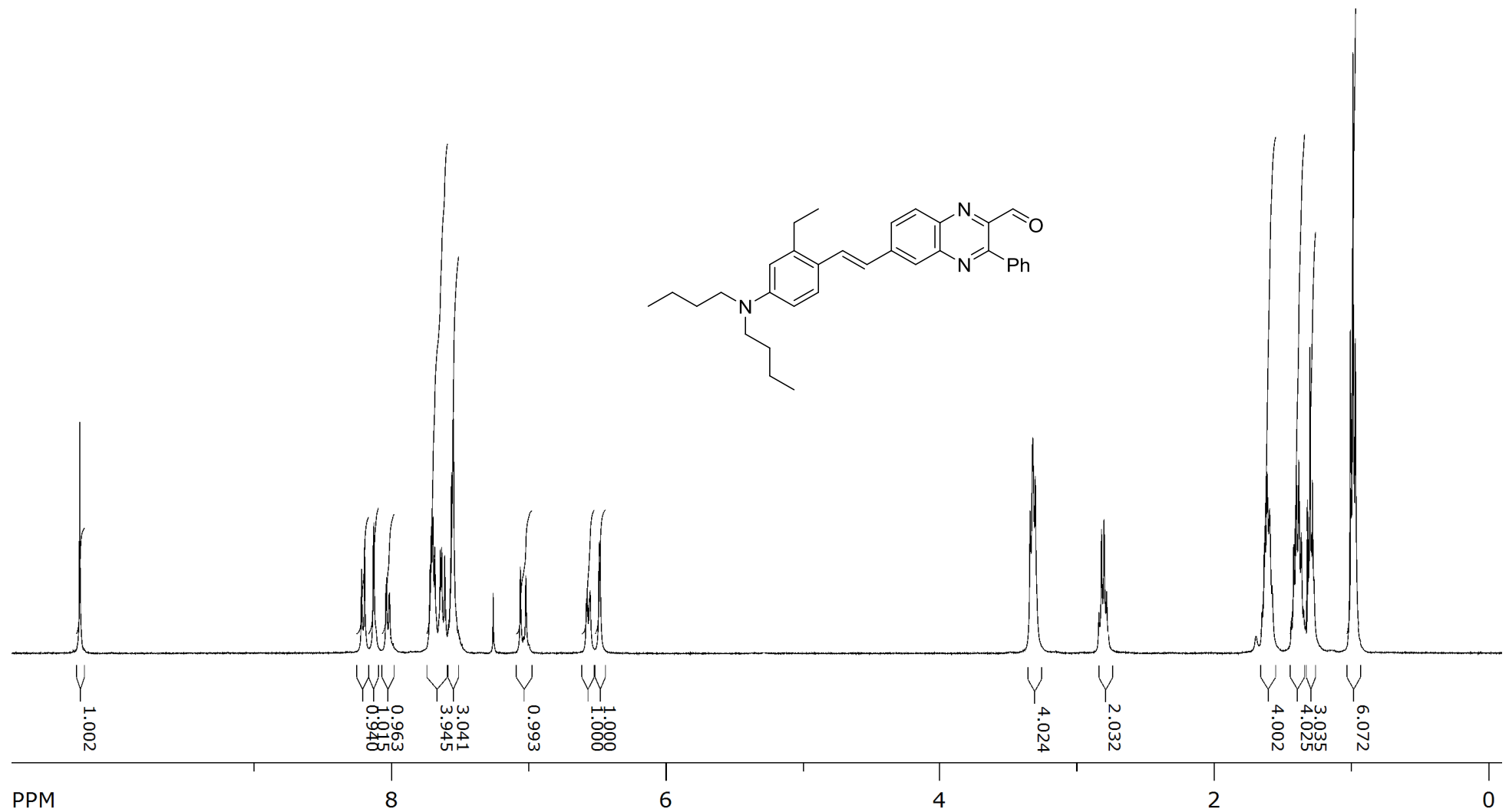
<sup>13</sup>C NMR spectrum (CDCl<sub>3</sub>, 100 MHz) of (*E*)-6-(4-(*N,N*-diethylamino)-2-(hexyloxy)styryl)-3-phenylquinoxaline-2-carbaldehyde (**4c**)



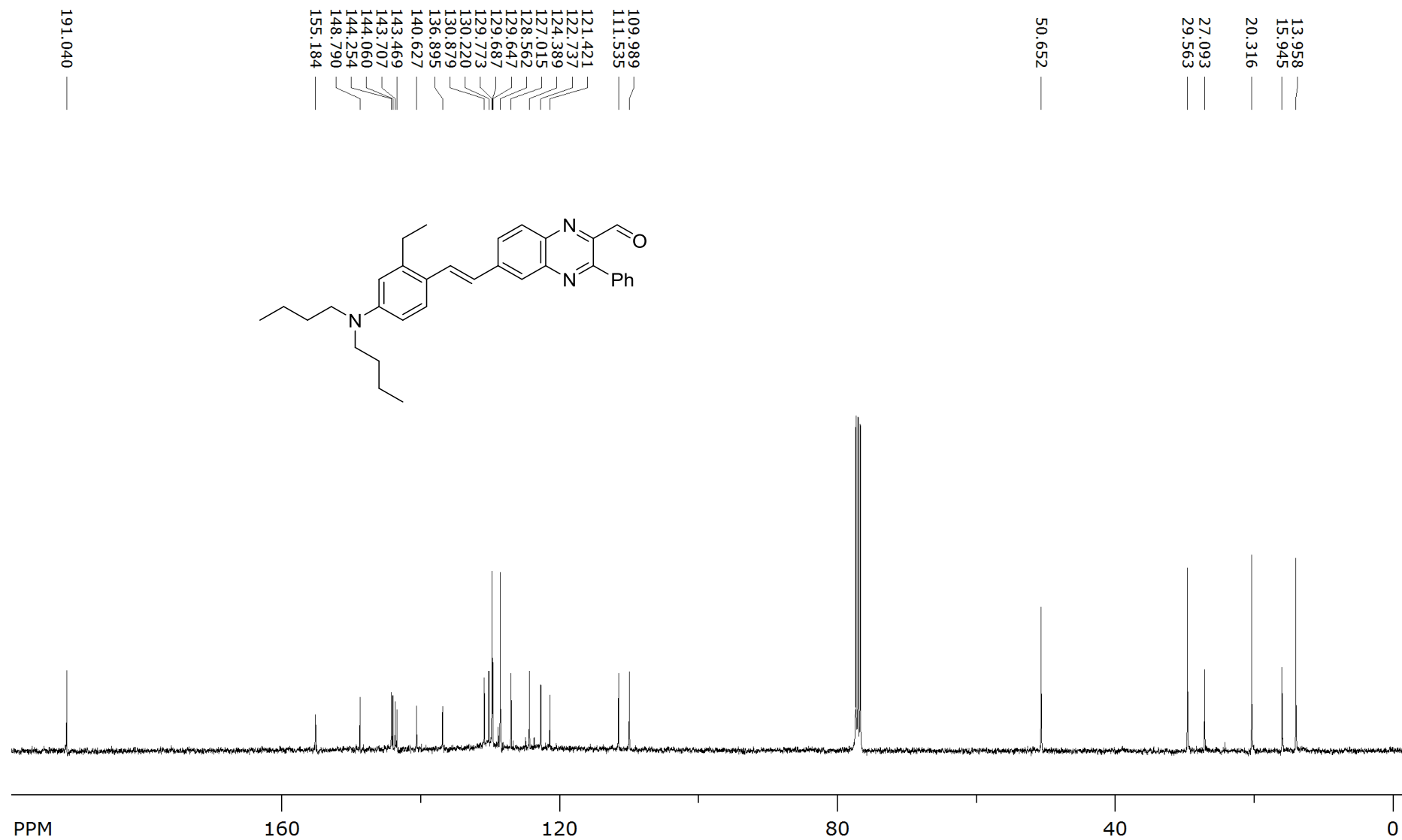


<sup>13</sup>C NMR spectrum (CDCl<sub>3</sub>, 100 MHz) of 2-(3-cyano-4-((*E*)-2-(6-((*E*)-4-(*N,N*-diethylamino)-2-(hexyloxy)styryl)-3-phenylquinoxalin-2-yl)vinyl)-5,5-dimethylfuran-2(*5H*)-ylidene)malononitrile (**HODEA-VQV-TCF**)

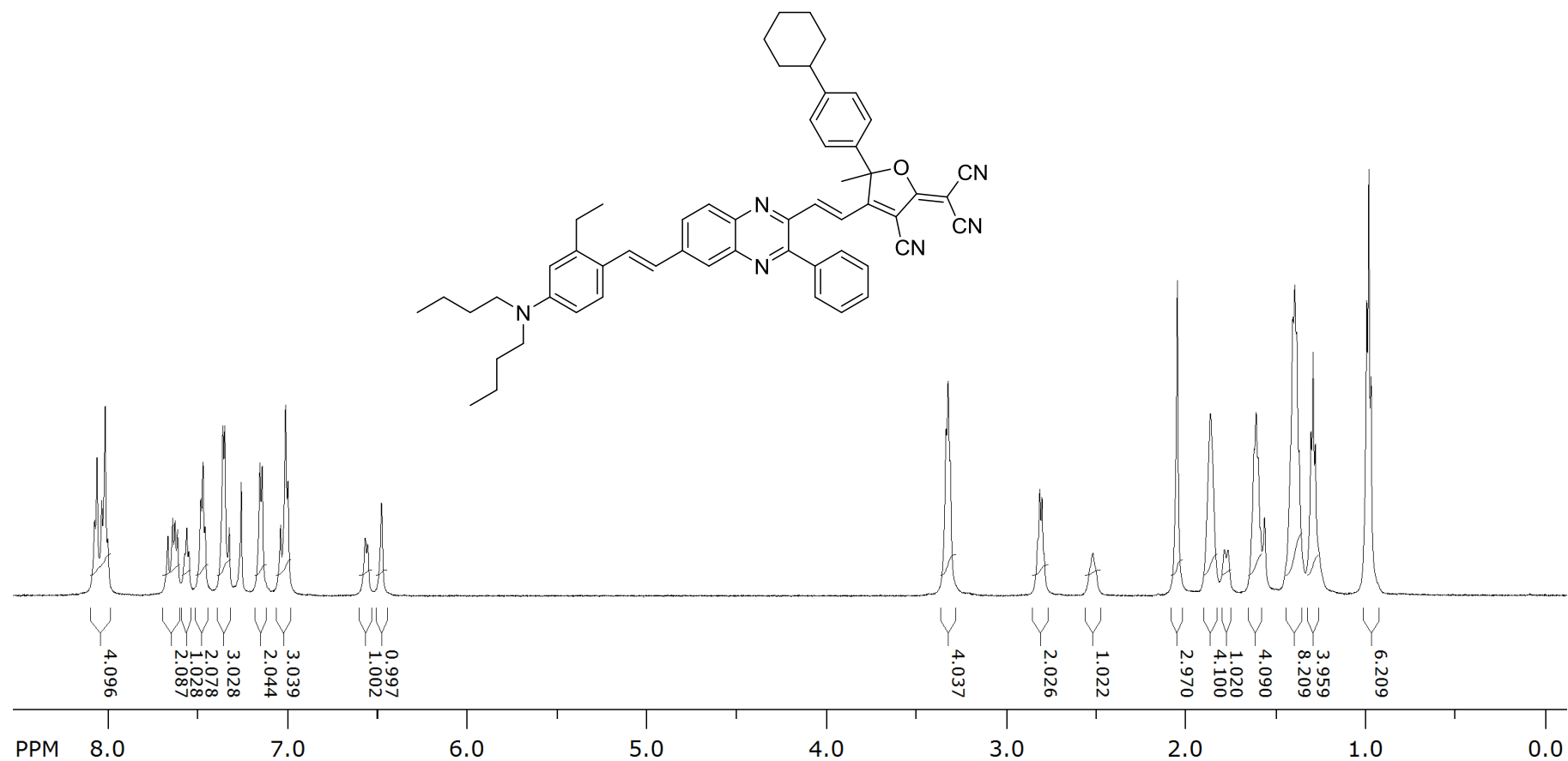




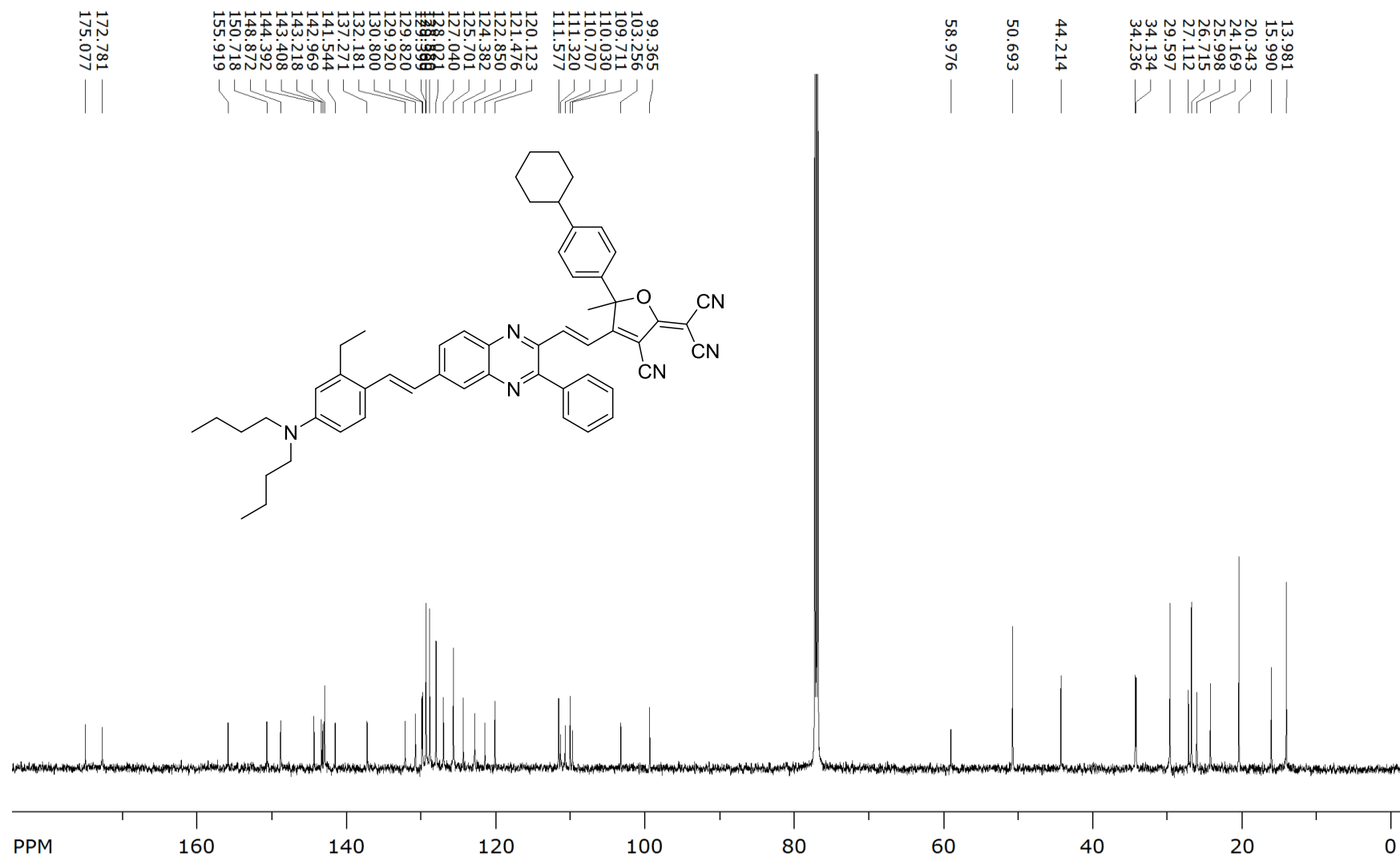
<sup>1</sup>H NMR spectrum (CDCl<sub>3</sub>, 400 MHz) of (*E*)-6-(4-(dibutylamino)-2-ethylstyryl)-3-phenylquinoxaline-2-carbaldehyde (**4a**)



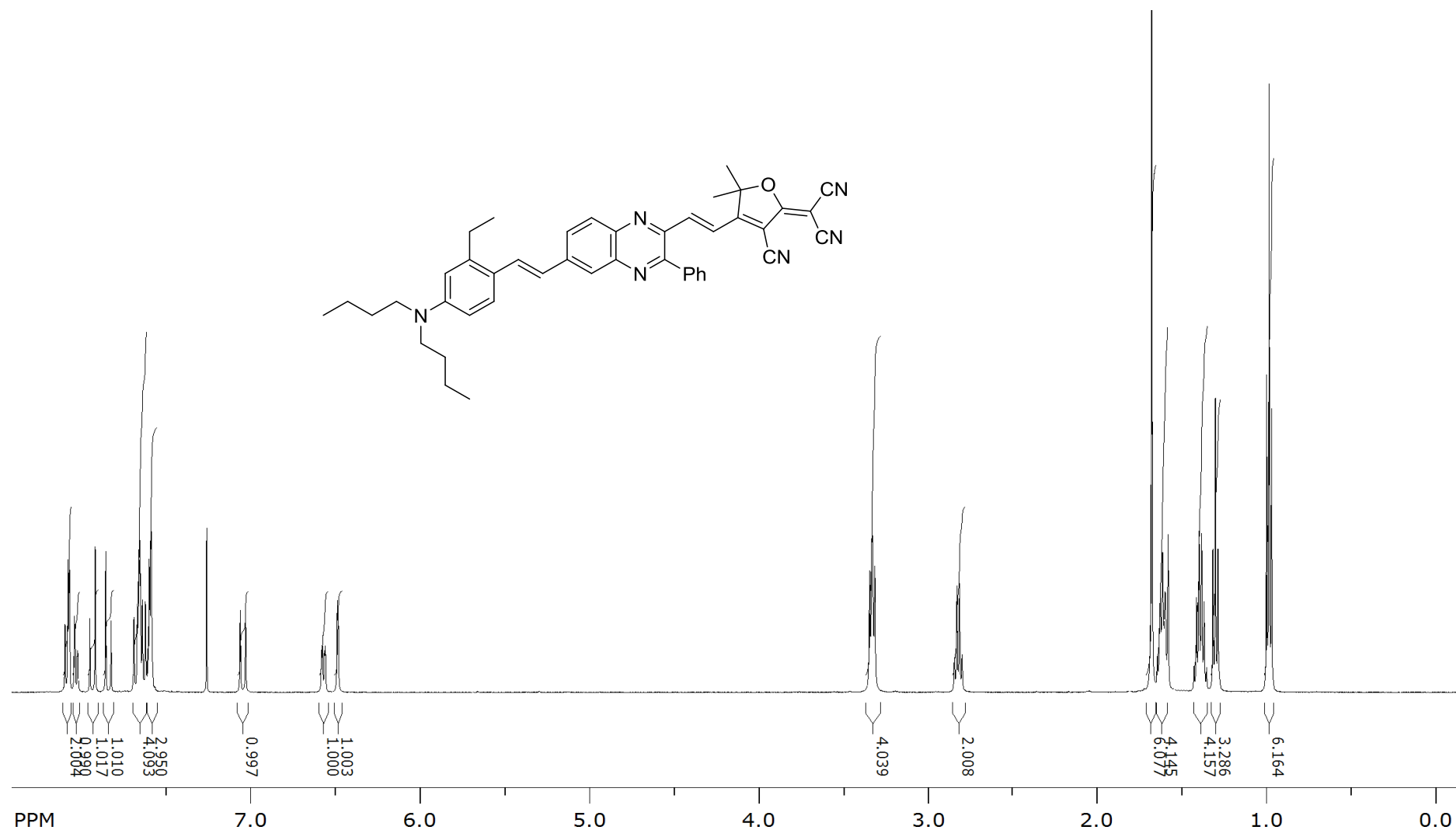
<sup>13</sup>C NMR spectrum (CDCl<sub>3</sub>, 100 MHz) of (E)-6-(4-(dibutylamino)-2-ethylstyryl)-3-phenylquinoxaline-2-carbaldehyde (**4a**)



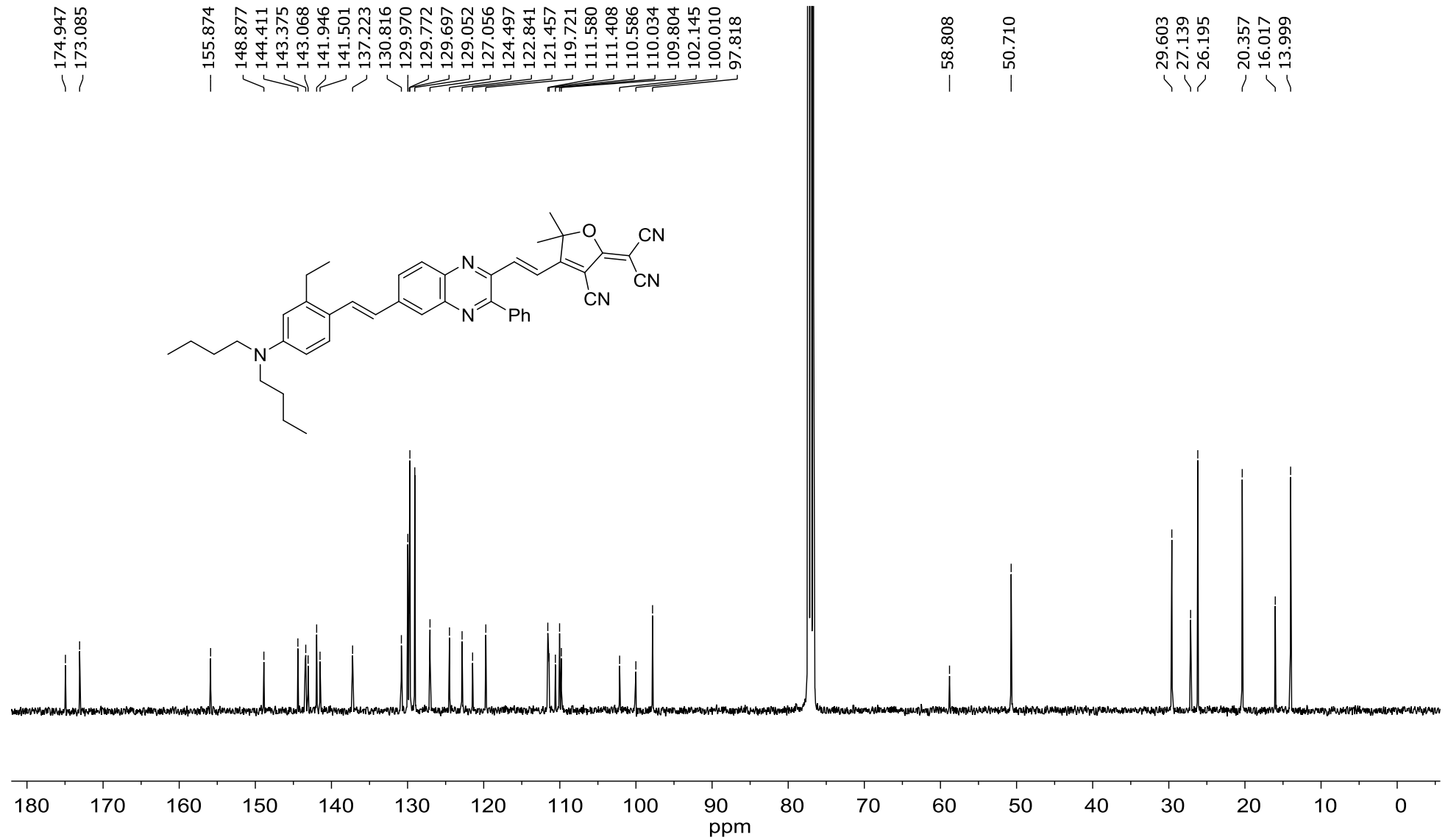
<sup>1</sup>H NMR spectrum (CDCl<sub>3</sub>, 600 MHz) of 2-(3-cyano-5-(4-cyclohexylphenyl)-4-((*E*)-2-(6-((*E*)-4-(dibutylamino)-2-ethylstyryl)-3-phenylquinoxalin-2-yl)vinyl)-5-methylfuran-2(*5H*)-ylidene)malononitrile (**EDBA-VQV-TCF<sub>PhCy</sub>**)



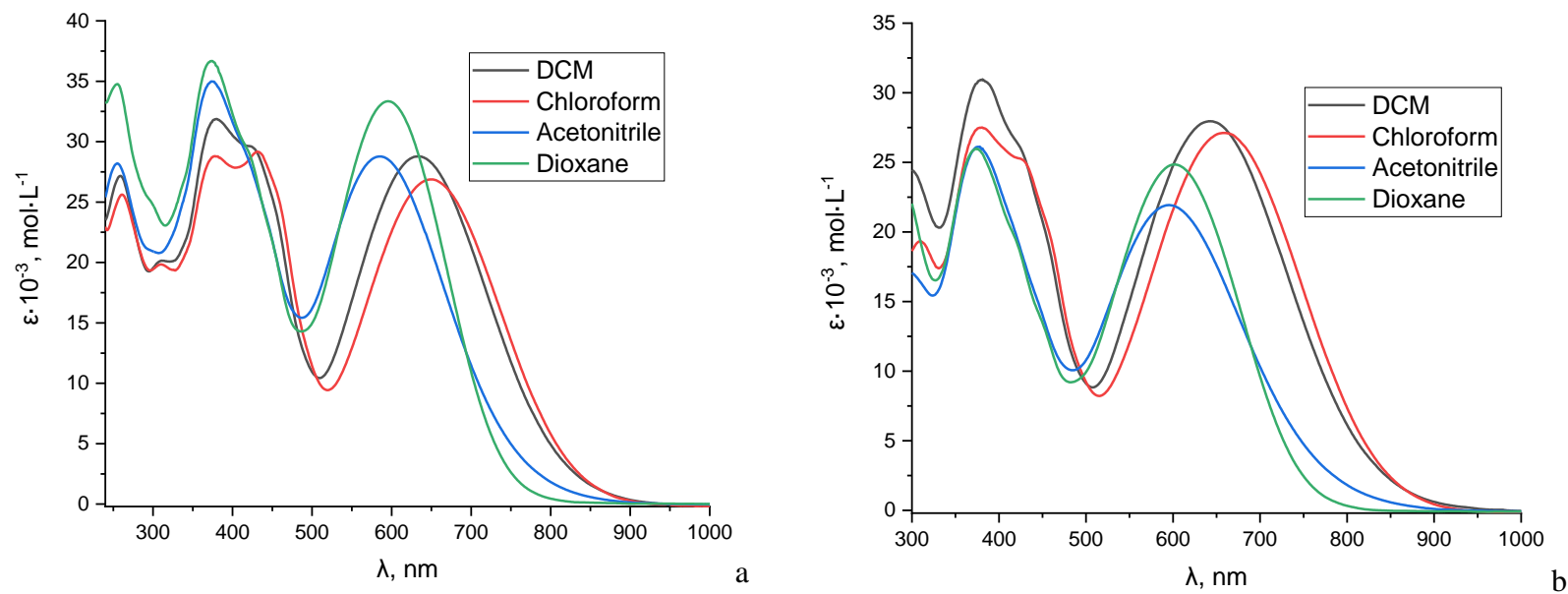
$^{13}\text{C}$  NMR spectrum ( $\text{CDCl}_3$ , 150 MHz) of 2-(3-cyano-5-(4-cyclohexylphenyl)-4-((*E*)-2-(6-((*E*)-4-(dibutylamino)-2-ethylstyryl)-3-phenylquinoxalin-2-yl)vinyl)-5-methylfuran-2(5H)-ylidene)malononitrile (**EDBA-VQV-TCF<sub>PhCy</sub>**)



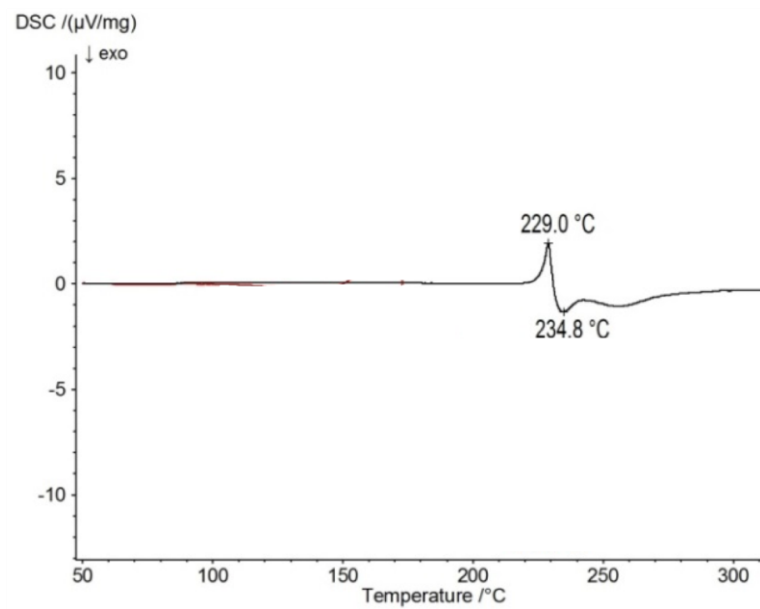
<sup>1</sup>H NMR spectrum (CDCl<sub>3</sub>, 500 MHz) of 2-(3-cyano-4-((E)-2-(6-((E)-4-(dibutylamino)-2-ethylstyryl)-3-phenylquinoxalin-2-yl)vinyl)-5,5-dimethylfuran-2(5H)-ylidene)malononitrile (**EDBA-VQV-TCF**)



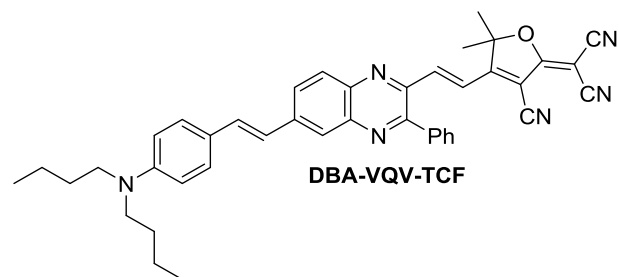
<sup>13</sup>C NMR spectrum (CDCl<sub>3</sub>, 100 MHz) of 2-(3-cyano-4-((E)-2-(6-((E)-4-(dibutylamino)-2-ethylstyryl)-3-phenylquinoxalin-2-yl)vinyl)-5,5-dimethylfuran-2(5H)-ylidene)malononitrile (EDBA-VQV-TCF).



**Figure S1.** Experimental electronic absorption spectra of **EDBA-VQV-TCF** (a), **HODEA-VQV-TCF** (b).



**Figure S2.** DSC curve for chromophores **DBA-VQV-TCF**<sup>21b</sup>





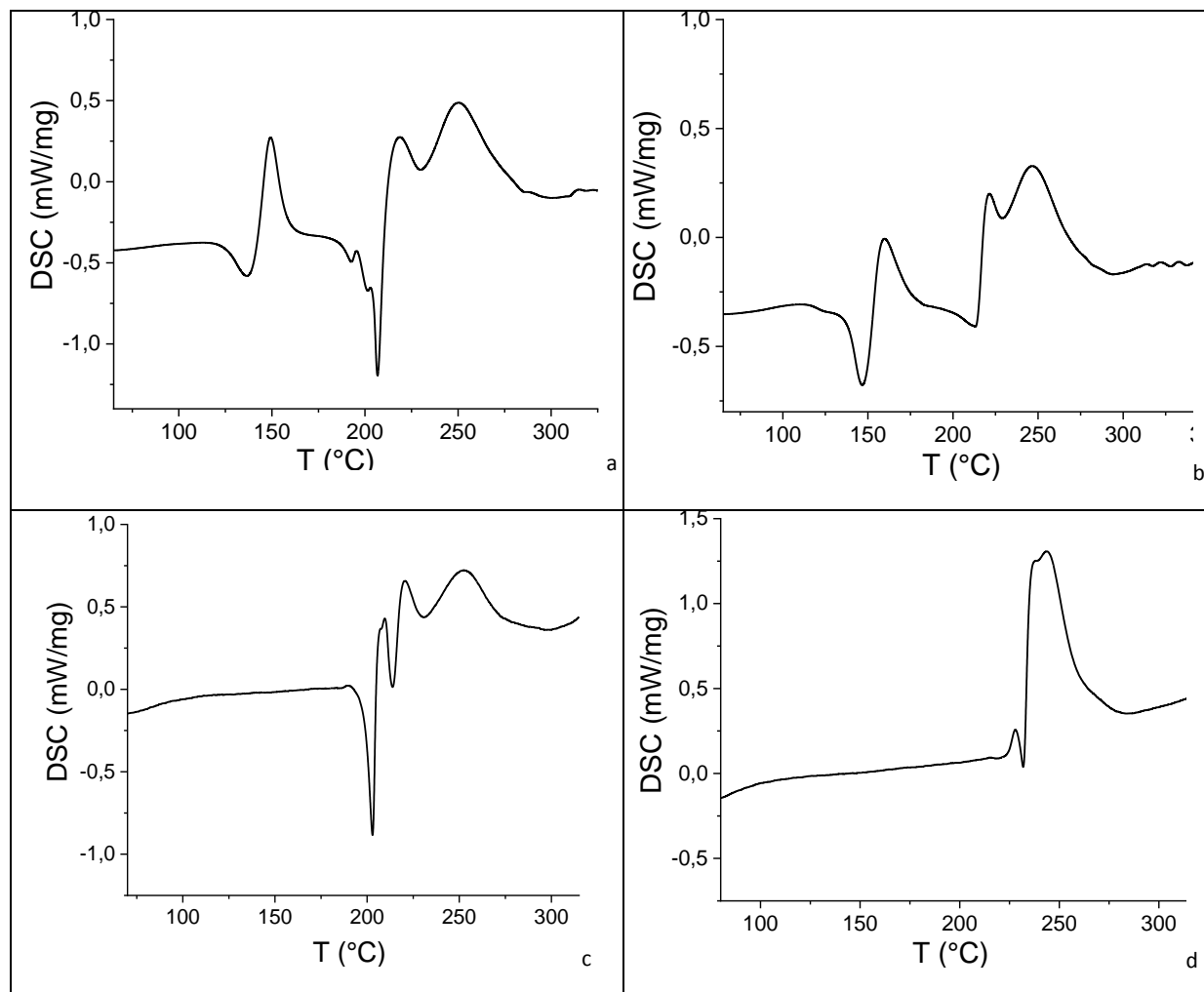


**Figure S3.** DSC curves for chromophores **HODEA-VQV-TCF** (a), **BODEA-VQV-TCF** (b), **EDBA-VQV-TCF** (c), **EDBA-VQV-TCF<sub>PhCy</sub>** (d) (endo ↓).

### Molecular modeling and DFT calculations

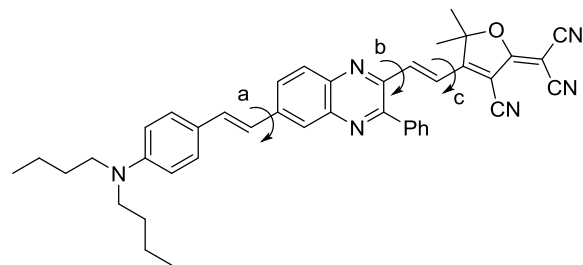


**Figure S4.** The notation of the bonds around which rotation is realized.

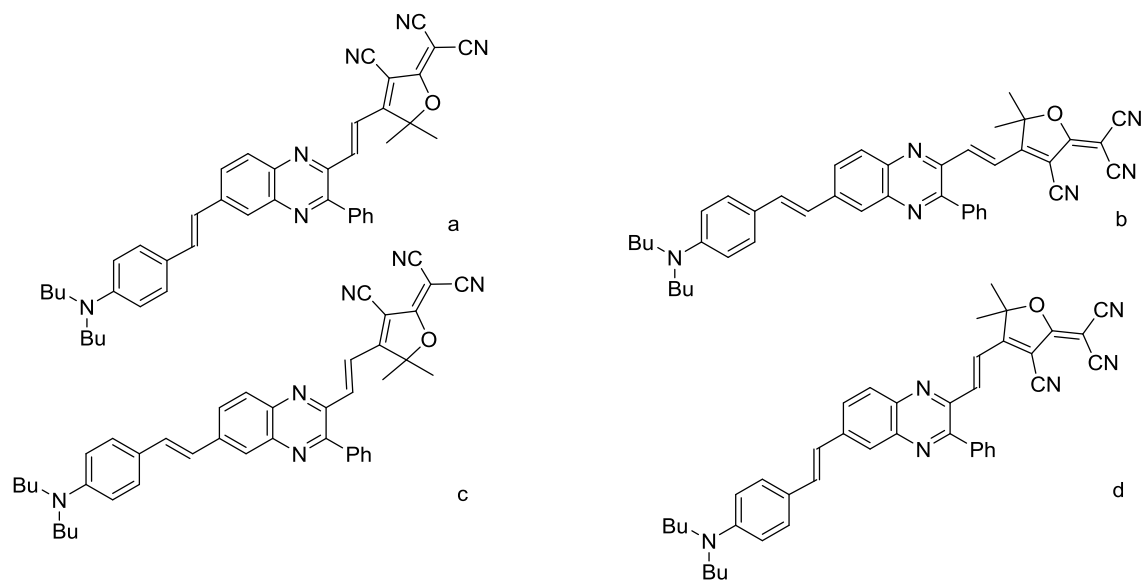


**Figure S5.** DBA-VQV-TCF conformers and their first hyperpolarizability values along with Boltzmann weight factors estimated by Conformational search:  $962 \cdot 10^{-30}$  esu (60.5%) (a);  $823 \cdot 10^{-30}$  esu (10.9%) (b);  $951 \cdot 10^{-30}$  esu (15.4%) (c);  $825 \cdot 10^{-30}$  esu (5.5%) (d). The analysis of the results of conformational search made it possible to identify the most stable and probable conformers *cct*, *ttt*, *tct* and *ccc* ones (summarized Boltzmann factors being 60.5, 10.9, 15.4, 5.5 %, respectively, for conformers in the energy window ca 2.2 kcal/mol). the corresponding values for *ttt*, *tct* and *ccc* conformers are  $823 \cdot 10^{-30}$  esu,  $951 \cdot 10^{-30}$  esu and  $825 \cdot 10^{-30}$  esu.

**Table S1.** Dihedral angles between moiety planes in **HODEA-VQV-TCF**, **BODEA-VQV-TCF**, **EDBA-VQV-TCF** and **EDBA-VQV-TCF<sub>PhCy</sub>**.

Dihedral angles	<b>HODEA-VQV-TCF</b>	<b>BODEA-VQV-TCF</b>	<b>EDBA-VQV-TCF</b>	<b>EDBA-VQV-TCF<sub>PhCy</sub></b>	<b>DBA-VQV-TCF</b>
$\varphi 1^a, ^\circ$	4.5	4.1	6.0	13.7	10.9
$\varphi 2^b, ^\circ$	3.5	3.5	2.4	3.8	3.3
$\varphi 3^c, ^\circ$	16.5	17.3	12.7	29.0	11.7
$\varphi 4^d, ^\circ$	21.0	21.3	17.9	41.6	20.1

<sup>a</sup> angle between the plane of donor fragment and the plane of closest ring of  $\pi$ -bridge;

<sup>b</sup> angle between the planes of fused rings in quinoxaline moiety;

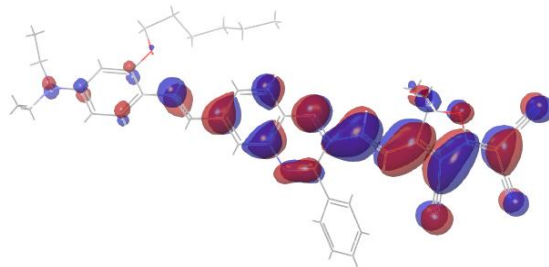
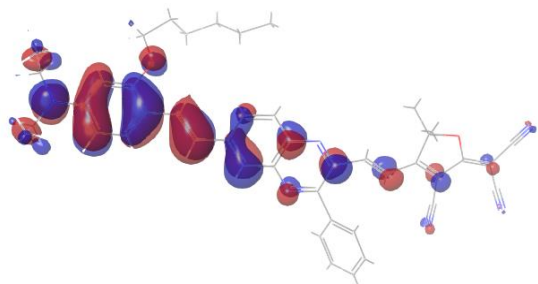
<sup>c</sup> between the TCF plane and the plane of the closest ring of quinoxaline moiety;

<sup>d</sup> angle between the planes of donor and acceptor moieties.

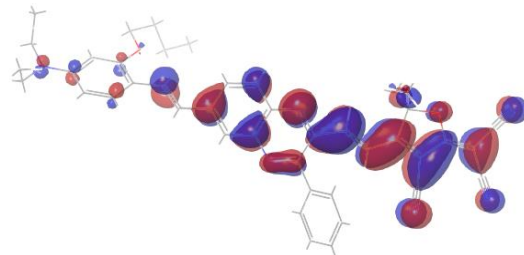
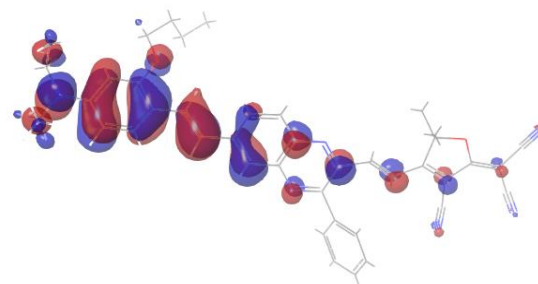
HOMO

LUMO

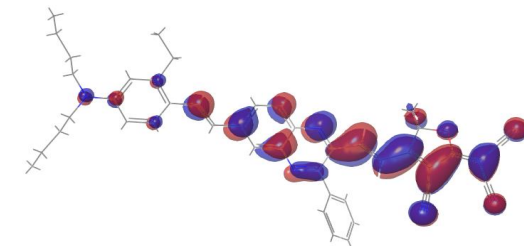
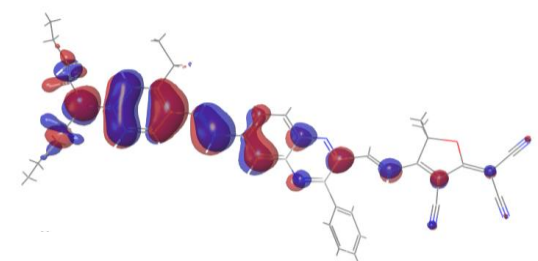
a



b



c



d

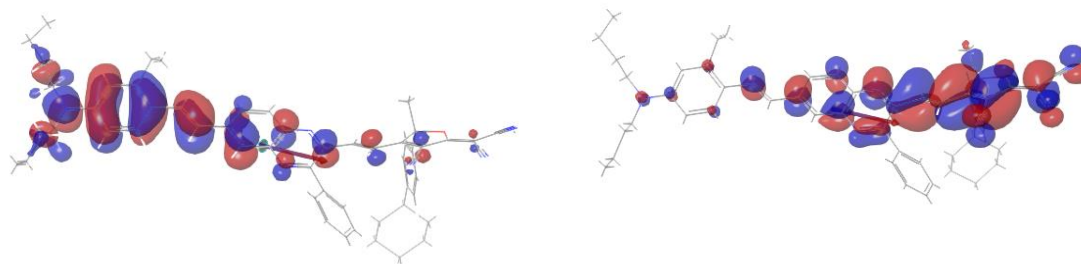


**Figure S6.** Frontier orbitals calculated at B3LYP/6-31G\* level: **HODEA-VQV-TCF (a)**, **BODEA-VQV-TCF (b)**, **EDBA-VQV-TCF (c)** and **EDBA-VQV-TCF<sub>PhCy</sub> (d)**.

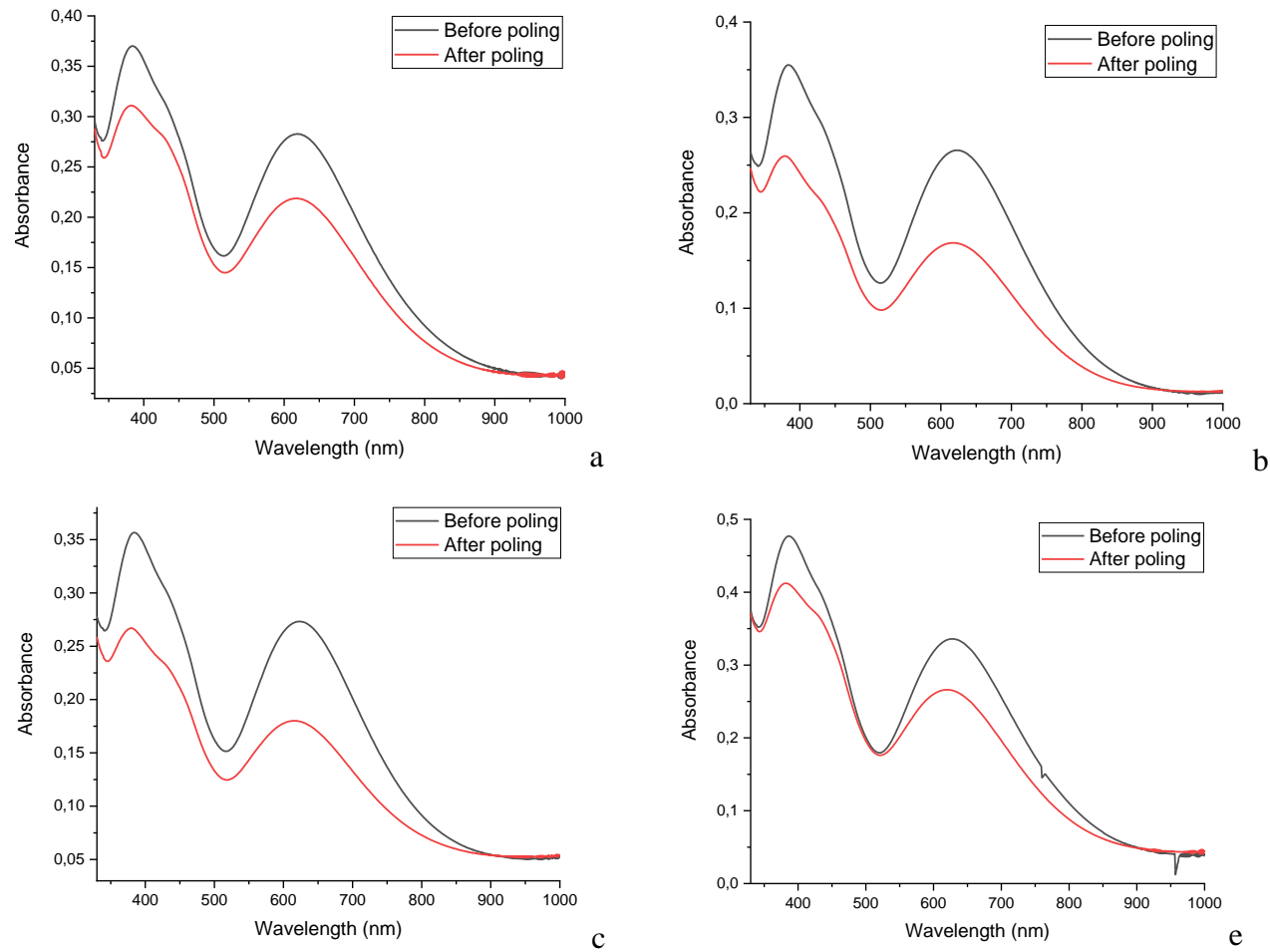


**Figure S7.** UV-Vis electron absorption spectra for **EDDBA-VQV-TCF(20)/PMMA** (a), **EDDBA-VQV-TCF(25)/PMMA** (b), **EDDBA-VQV-TCF(30)/PMMA** (c) and **EDDBA-VQV-TCF(35)/PMMA** (d) films before and after poling

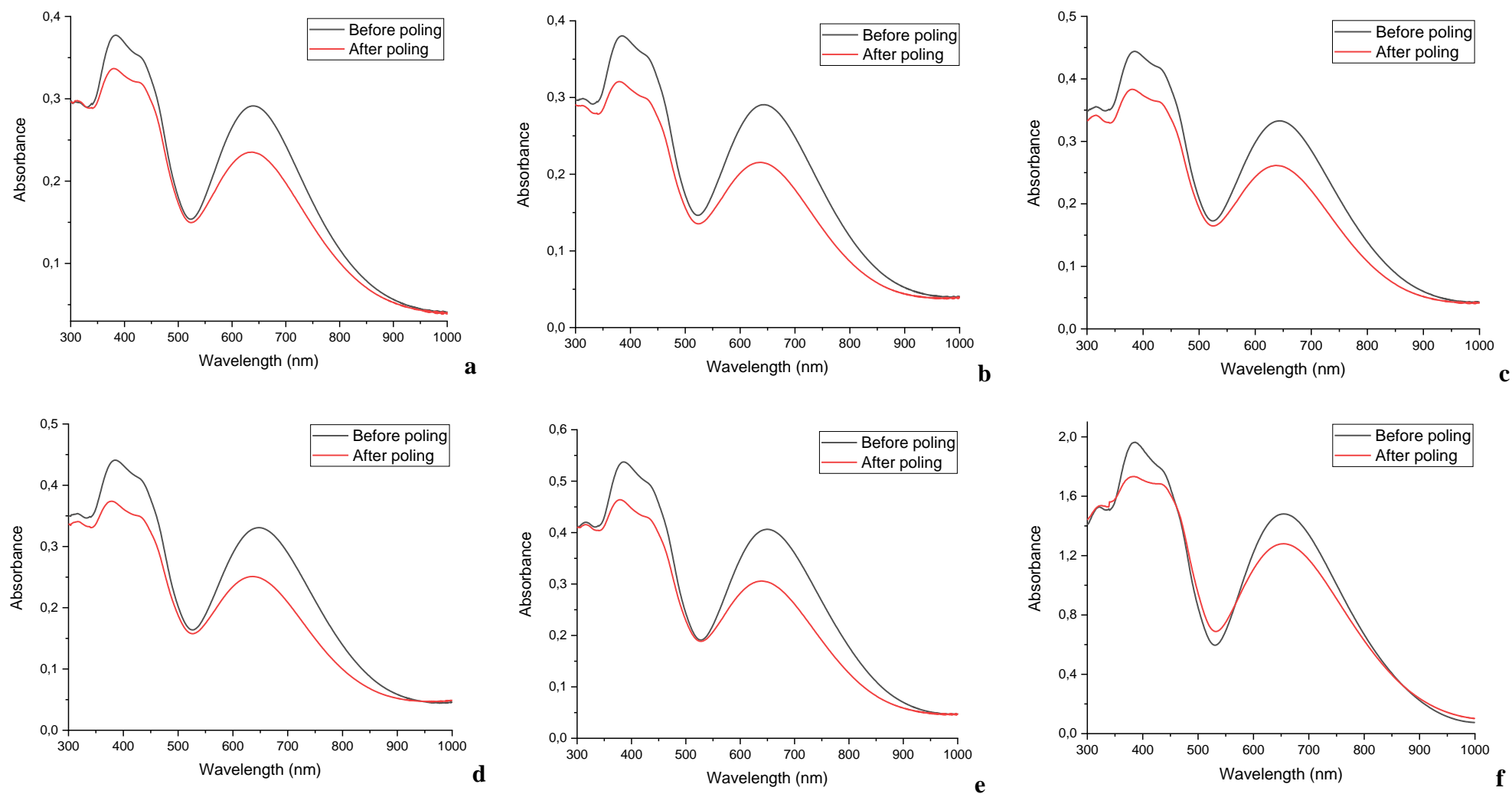


**Figure S8.** UV-Vis electron absorption spectra for EDBA-VQV-TCF<sub>PhCy</sub>(25)/PMMA (a), EDBA-VQV-TCF<sub>PhCy</sub>(30)/PMMA (b), EDBA-VQV-TCF<sub>PhCy</sub>(35)/PMMA (c), EDBA-VQV-TCF<sub>PhCy</sub>(40)/PMMA (d), EDBA-VQV-TCF<sub>PhCy</sub>(50)/PMMA (e) and EDBA-VQV-TCF<sub>PhCy</sub>(100%)/PMMA (f) films before and after poling

**Table S2.** NLO coefficients ( $d_{33}$ ), order parameters ( $\eta$ ),  $\lambda_{\max}$  of polymer film and film thickness ( $h$ ); poling temperature 110 °C.

Sample, Chromophore (load, wt%)/polymer	$h$ , nm	$\lambda$ , nm	$\eta$	$d_{33}^a$ , pm/V
<b>EDBA-VQV-TCF(20)/PMMA</b>	320	619	0.25	35
<b>EDBA-VQV-TCF(25)/PMMA</b>	200	617	0.33	50
<b>EDBA-VQV-TCF(30)/PMMA</b>	220	621	0.25	50
<b>EDBA-VQV-TCF(35)/PMMA</b>	250	628	0.30	33
<b>BODEA-VQV-TCF(25)/PMMA</b>	440	622	0.22	36
<b>BODEA-VQV-TCF(30)/PMMA</b>	600	627	0.24	40
<b>HODEA-VQV-TCF(25)/PMMA</b>	610	627	0.1	40
<b>HODEA-VQV-TCF(30)/PMMA</b>	430	625	0.23	51
<b>DBA-VQV-TCF/(25)PMMA</b>	372	610	0.26	39

<sup>a</sup> Estimated values (SHG experiment with approximate formula<sup>27a</sup>)



**Table S3.** NLO coefficients ( $d_{33}$ ), order parameters ( $\eta$ ), poling temperature ( $T_p$ ),  $\lambda_{\max}$  of polymer film and film thickness ( $h$ ) for composite material **EDBA-VQV-TCF<sub>PhCy</sub>/PMMA**.

chromophore load, wt%	$h$ , nm	$\lambda$ , nm	$T_p$ , °C	$\eta$	$d_{33}$ , <sup>a</sup> pm/V
25	340	639	100	0.21	40
30	290	644	110	0.28	50
35	300	647	110	0.24	52
40	270	647	110	0.29	62
50	260	649	110	0.28	47
100	560	655	110	0.10	37
100	480	660	133	0.17	44

<sup>a</sup> Estimated values (SHG experiment with approximate formula<sup>27a</sup>)